Hjelstuen, B.O., and Sejrup, H.P., 2020, Latitudinal variability in the Quaternary development of the Eurasian ice sheets—Evidence from the marine domain: Geology, v. 49, https://doi.org/10.1130/G48106.1

Latitudinal variability in the Quaternary development of the Eurasian Ice Sheets - evidence from the marine domain

Berit Oline Hjelstuen and Hans Petter Sejrup

Department of Earth Science, University of Bergen, Allegt 41, N-5007 Bergen, Norway

Supplemental Material

RESULTS OF DATA COMPILATION

The compiled *Quaternary isopach map* (Fig. 1) is based on merging of previously published isopach maps from the NE Atlantic margin, from Ireland to Svalbard (Faleide et al., 1996; Stoker et al., 2005; Dowdeswell et al., 2010; Ottesen et al., 2012), the North Sea (Ottesen et al., 2018) and the Yermak Plateau (Geissler et al., 2011) (Table S1; Fig. S1). Except for in the region at the mouth of the Kveithola Trough (Lasabuda et al., 2018) no Quaternary isopach map exist in the Nansen Basin, Arctic Ocean. Mapping of Quaternary sediments in the Nansen Basin is, therefore, based on extracting sediment thickness information from published 2D seismic profiles (Geissler and Jokat, 2004; Jokat and Micksch, 2004; Nikishin et al., 2018) (Fig. S1; Fig. S2, Table S1). Likewise, the thickness map in the Norway Basin (Fig. 1, Fig. S1) is generated from published seismic profiles (Hjelstuen and Andreassen, 2015) and new interpretation of 2D seismic profiles that have been accessible through the DISKOS database (www.diskos.no). Available information from ODP/DSDP sites and shallow borings (Fig. S1) have also been used in order to justify and identify Quaternary sediment thicknesses. Depth conversion, from depth in time to depth in meters, have been performed by using sediment velocities presented in the published papers, or by using information from nearby regions with similar geological setting.

The *chronostratigraphy* of the pre-Last Glacial Maximum Quaternary sediment package in the region is to a large degree based on paleomagnetic studies, micropaleontology, $^{86/87}Sr$ and to some degree amino acid geochronology. The 2.6 Ma and 0.78 Ma NHG phase boundaries presented in our study represent the Matuyama/Gauss and Brunhes-Matuyama paleomagnetic boundaries, whereas the NHG Phase III boundary is based on paleomagnetic excursion events Top Olduvai (1.77 Ma) and Base Jaramillo (1.0 Ma) and biostratigraphy. These paloemagnetic boundaries and excursions have been identified in a number of deep sea cores and shallow drillings in the studied region (Fig. S1; Table S2).

It should be noted that in the northern Nansen Basin, Arctic Ocean, the chronostratigraphy is based on downlap of sequence boundaries onto oceanic basement of known age (Nikishin et al., 2018). As no Base Late Pleistocene boundary has been identified in this region the Miocene sequence boundary has been used when generating the Quaternary isopach map (Fig. 1, Fig. S2). Thereby, the Quaternary sediment thicknesses should be considered a maximum value. However, likewise to the other margin segments investigated in this study, we assume that the Miocene sediment input to the Arctic Ocean margin is very low compared to the sediment volumes deposited during the last 2.6 million years. In the North Sea TMF the Base Late Pleistocene boundary is also rather poorly constrained. We consider Stoker et al. (2005) to have the most reliable mapping of the Base Late Pleistocene sequence boundary in this region.

Published *ice-rafted debris* (IRD) records from the Yermak Plateau, the Fram Strait, the Mid-Norwegian and the British-Irish margins have been compiled (Fig. S3). The IRD records presented are all located nearby the paleo-EurIS marine margin, and is thus suggested to reflect size-variations in the KBIS (ODP sites 911, 908/909, 987), FIS (ODP sites 643, 644) and BIIS (IODP Site U1317E). It should be noted that the records are shown in weight percent, number of IRD grains etc. In addition, different grain sizes (>2 mm, >0.5 mm, >0.125 mm), has also been used.

Lastly, we have compiled *glacial landform* evidences of the existence of the EurIS (Table S3). Such evidences are Mega-Scale Glacial Lineations (MSGLs), formed beneath ice streams, and Glacigenic Debris Flows (GDFs), which are related to shelf-edge glaciations and ice streaming.

SEDIMENT VOLUME AND SEDIMENTATION RATE ESTIMATES - METHODS

Quaternary sediment volumes and sedimentation rates

In order to estimate sediment volumes the "extract by mask" and "surface volume" tools in the ArcGIS software (version 10.6) have been used. For this, the mid-oceanic spreading centers (Fig. 1) define the 0-m-thickness contour. Quaternary sediment volumes were first estimated for each margin segment (Table S4a) and then these sediment volumes were summed to represent erosion products derived from the KBIS, FIS and BIIS ice sheets (Table S4b). An average Quaternary sediment (dry) density of 1.80 g/cm^3, as estimated by Hjelstuen et al. (1996) and Fielder and Faleide (1996), has been used for converting sediment volumes into weight in tons.

For each main depocentre along the EurIS marine margin average Quaternary sedimentation rates (Table S5) have been estimated by using the above-described ArcGIS procedure, delineating the depositional area by the 200 m thickness contour (except for the Donegal TMF) and by utilizing the equation: *(sediment volume / depositional area) : year*. Maximum rates (Table S5) are also estimated by reading off maximum thickness in each depocentre from the ArcGIS-extracted isopach map.

Due to sparse age control in the northern part of the Arctic Ocean the Quaternary sediment volume should be considered an absolute maximum in this region. Elsewhere along the paleo-EurIS marine margin the sediment volume is anticipated rather well constrained. We have defined a 0-m contour along the shelf edge and along the mid-oceanic ridge. This is also considered reliable, as e.g. seismic profiles across TMF systems along the western Svalbard-Barents Sea margins (Fig. S2) clearly show that they are terminating toward the oceanic spreading center.

Preglacial (55-2.7 Ma) sedimentation rates

The pre-glacial sedimentation rates are, in regions where isopach maps exits (e.g. the western Barents Sea), based on estimated sediment volumes and depositional areas presented in published papers (Table S6). Elsewhere, such estimates are based on published seismic profiles and/or isopach maps, using sediment thickness information from the shelf edge regions. In Table S6 the method used to estimate sedimentation rates ("average" - based on sediment volumes and depositional areas and/or "linear" – based on seismic profiles and/or isopach maps) are indicated.

Sedimentation rates and sediment discharge – the three glacial phases

Commonly, in regions where isopach maps have been published for the three NHG phases defined in this study (e.g. Dowdeswell et al., 2010; Anell et al., 2012) information on sediment volumes, sediment thicknesses and depositional area have been estimated and corresponding average sedimentation rates and sediment discharge values have been calculated. In the present paper we use this information directly or if a new chronostratigraphy (Table S1) have been utilized, as for e.g. the western Barents Sea margin, average sediment rates and sediment discharge has been recalculated (Tables S6, S7). In areas where the above-mentioned information does not exist, shelf edge sediment thicknesses in published seismic profiles have been used.

Table S1. Previously published information used in this study. *Column 1 (from left)*: Number refer to number as annotated in Fig. S1 which show study area of the published papers listed in this table. *Column 2*: Study area/region in actual paper. *Column 3:* Figures and/or information from tables which have been used in present study. *Column 4*: Chronostratigraphic framework which has been used in present study. *Column 5*: Sediment velocities used in order to depth convert (to depth in meter) seismic profiles and/or isopach maps. *Column 5*: Information in the actual paper has been used: (i) to generate the Quaternary isopach map (QM), (ii) to estimate Quaternary sedimentation rates (GR), (iii) to estimate pre-Quaternary Cenozoic sedimentation rates (PR) or (iv) as background and/or supporting information (BI). *Column 6*: Authors of the published papers listed in this table.

Table S1-A. East Arctic Ocean margin

Id (Fig. S1)	Region	Figure - Table	Chronology (based on)	Sediment velocities	Used for	Reference
1	Nansen Basin	Fig. 5, 6	Used chronology as presented in paper (Downlap of sequence boundaries on oceanic basement)	Velocities as given in paper	QM, GR, PR	Nikishin et al (2018)
2	Nansen Basin	Fig. 2	Used chronology as presented in paper (Regional seismic stratigraphy, ODP sites)	N/A	QM	Jokat and Micksch (2004)
3	Nansen Basin	Fig. 8	Used chronology as presented in paper (Fig. 13)	Velocities as given in paper	QM	Engen et al. (2009)
4	Yermak Plateau	Fig. 17a	Used chronology as presented in paper (Regional seismic stratigraphy, ODP sites)	Velocities as given in paper	QM	Geissler et al. (2011)
5	Yermak Plateau	Fig. 3-6, 8-11	Used chronology as presented in paper (Regional seismic stratigraphy, ODP sites)	Velocities as given in paper	QM	Geissler and Jokat (2004)
6	Yermak Plateau	N/A	Used chronology as presented in paper (Regional seismic stratigraphy, ODP sites)	N/A	BI	Fransner et al. (2018)
7	N Svalbard Margin	Table 1, 2	Used chronology as presented in paper (Regional seismic stratigraphy, ODP sites)	N/A	GR	Lasabuda et al. (2018)
8	Fram Strait	Fig. 3-5	Used chronology as presented in paper (Regional seismic stratigraphy, ODP sites)	1800 m/s (Geissler et al. 2011)	QM	Gebhardt et al. (2014)

Table S1-B. Western Svalbard margin

Id (Fig. S1)	Region	Figure - Table	Chronology (based on)	Sediment velocities	Used for	Reference
9	Sjubrebanken TMF	Fig. 11	Used chronology presented in paper (Regional seismic stratigraphy, ODP sites 911 and 986)	1800 m/s (Geissler et al. 2011)	QM	Sarkar et al. (2011)
10	Sjubrebanken TMF	Fig. 6	Used chronology presented in paper (ODP sites 910-912)	1800 m/s (Geissler et al. 2011)	GR, PR	Mattingsdal et al. (2014)
9	Kongsfjorden TMF	Fig. 11	Used chronology presented in paper (Regional seismic stratigraphy, ODP sites 911 and 986)	1800 m/s (Geissler et al. 2011)	QM	Sarkar et al. (2011)
10	Kongsfjorden TMF	Fig. 6	Used chronology presented in paper (ODP sites 910-912)	1800 m/s (Geissler et al. 2011)	GR, PR	Mattingsdal et al. (2014)
11	Isfjorden TMF	Fig. 14	Use revised chronology by Laberg et al. (2010; 2012)	2000 m/s (Solheim et al., 1998)	QM	Faleide et al. (1996)
12	Isfjorden TMF	Fig. 3	Use revised chronology by Laberg et al. (2010; 2012) (Knies et al. (2009), paleomagnetism, amino acid)	2000 m/s (Solheim et al., 1998)	BI	Solheim et al. (1996)
13	Isfjorden TMF	Fig. 3a	Use revised chronology by Laberg et al. (2010; 2012) (Knies et al. (2009), paleomagnetism, amino acid)	2000 m/s (Solheim et al., 1998)	GR, PR	Amundsen et al. (2011)
11	Bellsund TMF	Fig. 14	Use revised chronology by Laberg et al. (2010; 2012) (Knies et al. (2009), paleomagnetism, amino acid)	2000 m/s (Solheim et al., 1998)	QM	Faleide et al. (1996)
12	Bellsund TMF	Fig. 3	Use revised chronology by Laberg et al. (2010; 2012) (Knies et al. (2009), paleomagnetism, amino acid)	2000 m/s (Solheim et al., 1998)	BI	Solheim et al. (1996)
13	Bellsund TMF	Fig. 6a	Use revised chronology by Laberg et al. (2010; 2012) (Knies et al. (2009), paleomagnetism, amino acid)	2000 m/s (Solheim et al., 1998)	GR, PR	Amundsen et al (2011)

Table S1-C. Western Barents Sea margin

Id (Fig. S1)	Region	Figure - Table	Chronology	Sediment velocities	Used for	Reference
14	Storfjorden TMF	Fig. 9, Table 2	Use revised chronology by Laberg et al. (2010; 2012) (Knies et al. (2009), paleomagnetism, amino acid)	This study has already depth converted maps	QM, GR, PR	Hjelstuen et al. (1996)
15	Bjørnøyrenna TMF	Fig. 6, Table 2	Use revised chronology by Laberg et al. (2010; 2012) (Knies et al. (2009), paleomagnetism, amino acid)	This study has already depth converted maps	QM, GR, PR	Fiedler and Faleide (1996)

Table S1-D. Norwegian margin

Id (Fig. S1)	Region	Figure - Table	Chronology	Sediment velocities	Used for	Reference
16	Mid Norwegian Margin	Fig. 1 and Table 1	Used chronology presented in paper	Velocities as given in paper	QM, GR	Dowdeswell et al (2010)
17	North Sea TMF (proximal)	Table 1 and Fig. 4 (dep area)	Used chronology presented in paper	Velocities as given in paper	GR, QM	Hjelstuen et al. (2012)
18	North Sea TMF (proximal)	Fig. 6c	Used chronology presented in paper	2000 m/s	QM	Stoker et al. (2005)
19	North Sea TMF (proximal)	Fig. 4	Used chronology presented in paper	2000 m/s	QM	Ottesen et al. (2012)
20	Norway Basin	Fig. 4b and new seismic interpretation	Used chronology presented in paper	Velocities as given in paper	GR (2.7-0.5 Ma), PR, QM	Hjelstuen and AnSeassen (2015)
17	Norway Basin	Table 1, new area estimates	Used chronology presented in paper	Velocities as given in paper	GR (0.5-0 Ma)	Hjelstuen et al. (2012)

Table S1-E. North Sea

Id (Fig. S1)	Region	Figure - Table	Chronology	Sediment velocities	Used for	Reference
21	North Sea	Fig. 4a, Table 1	Used chronology presented in paper	2000 m/s (1800 m/s used in paper to estimate volume)	QM, GR	Ottesen et al. (2018)
22	North Sea	Table 2	Used chronology presented in paper	Velocities as given in paper	PR	Anell et al. (2012)
23	North Sea	N/A	Used chronology presented in paper	N/A	BI	Sejrup et al. (1987)
24	North Sea	N/A	Used chronology presented in paper	N/A	BI	Sejrup et al. (1995)
25	North Sea	N/A	Used chronology presented in paper	N/A	BI	Sejrup et al. (2000)
26	North Sea	Table 2, Fig. 2	Used chronology presented in paper	Velocities as given in paper	GR	Reinardy et al. (2017)
27	North Sea	N/A	Used chronology presented in paper	N/A	BI	Reinardy et al. (2018)

Table S1-F. British-Irish North Atlantic margin

Id (Fig. S1)	Region	Figure - Table	Chronology	Sediment velocities	Used for	Reference
18	British-Irish margin	Fig. 6c & 6b	Used chronology presented in paper	2000 m/s	QM, GR, PR	Stoker et al. (2005)

Table S2. Identified magnetostratigraphic events at selected sites and shallow borings along the EurIS marine margin. B/M: Brunhes-Matuyama; M/G: Matuyama-Gauss

Site/Boring (Fig. S1)	Identified magnetostratigraphic events - Quaternary	Reference
ODP site 908	B/M boundary, Jaramillo Top, Jaramillo Base, Olduvai Top, Olduvai Base, M/G boundary	Myhre et al. (1995)
ODP Site 909	B/M boundary, Jaramillo Top, Jaramillo Base, M/G boundary	Myhre et al. (1995)
ODP Site 910	B/M boundary, Jaramillo Top, Jaramillo Base, Cobb Mountain Top	Myhre et al. (1995)
ODP Site 911	B/M boundary, Jaramillo Top, Jaramillo Base, Cobb Mountain Top, Olduvai Top, Olduvai Base, M/G boundary	Myhre et al. (1995)
ODP Site 986	B/M boundary, Jaramillo Top, Jaramillo Base, Olduvai Top, Olduvai Base, Reunion	Channell et al. (1999)
ODP Site 644	B/M boundary, Jaramillo Top, Jaramillo Base, Olduvai Top, Olduvai Base, M/G boundary	Eldholm et al. (1987)
ODP Site 643	B/M boundary, Jaramillo Top, Jaramillo Base, Olduvai Top, Olduvai Base, M/G boundary	Eldholm et al. (1987)
ODP Site 642	B/M boundary, Jaramillo Top, Jaramillo Base, Olduvai Top, Olduvai Base, M/G boundary	Eldholm et al. (1987)
77/2	B/M boundary, Jaramillo event	Stoker et al. (1983)
81/26	B/M boundary, Jaramillo event	Stoker et al. (1983), Sejrup et al. (1987)
89-03	B/M boundary, Jaramillo event, Cobb Mountain event	Sejrup et al. (1995)
Southern North Sea	Olduvai Top, Olduvai Base, Reunion, M/G boundary	Kuhlmann et al. (2006)

Table S3. Glacial landform evidences of ice sheets and ice streams, EurIS marine margin. Increased font size indicates "more prominent" and/or "increased effect". GDF: Glacigenic Debris Flows, ICE: Grounded ice erosion, P: Iceberg plough marks, M: Mega-scale glacial lineations.

Time period (Ma)	N Svalbard Margin[1]	NW Svalbard Margin[2,3]	W Svalbard Margin[4]	NW Barents Sea Margin[4]	SW Barents Sea Margin[5,6]	Mid-Norwegian margin[7]	North Sea TMF[8,9]	North Sea[10,11,12]
0.0 – 0.78	GDF	ICE	GDF	GDF	GDF	M, P	GDF	GDF, P, MSGL
0.78 – 1.0	GDF	ICE	GDF	GDF	GDF	M, P	GDF	GDF, P, MSGL
1.0 – 1.5	GDF	ICE	GDF	GDF	GDF	M, P	GDF	GDF, P, MSGL
1.5 – 2.0	GDF	GDF	GDF (from 1.8 Ma?)	GDF (from 1.8 Ma?)		M, P		GDF, P,MSGL
2.0 – 2.6	GDF	GDF				M, P		GDF, P

[1]Lasabuda et al. (2018), [2] Sakar et al. (2011), [3]Mattingsdal et al. (2014), [4]Solheim et al. (1998), [5]Laberg et al. (2010), [6]Waage et al. (2018), [7]Montelli et al. (2017), [8]Hjelstuen and Grinde (2016), [9]Nygård et al. (2005), [10]Ottesen et al. (2018), [11]Reinardy et al. (2017), [12]Rea et al. (2018)

Table S4 a. Estimated Quaternary sediment volumes for the different segments of the EurIS marine margin

Margin segment	Sediment volum (10^3 km^3)	Depositional area (10^3 km^2)	% sediment volum of total	Weight (10^{14} tons)
East Arctic Ocean margin	743	952	41	13,4
Western Svalbard-Barents Sea margin	591	476	33	10,6
Norway margin	265	619	15	4,8
Irish-British North Atlantic margin	46, 2	406	3	0,8
North Sea	143	326	8	2,6
North Sea (UK sector)	*53, 9*	*129*		
North Sea (Norwegian sector)	*89, 1*	*197*		
Totalt	1 788, 2	2 779	100	32,2

Table S4 b. Estimated Quaternary sediment volumes along the marine margins of the paleo-KBIS, paleo-FIS and paleo-BIIS ice sheets.

Ice sheet	Sediment volum (10^3 km^3)	Depositional area (10^3 km^2)	% sediment volum of total	Weight (10^{14} tons)
KBIS	1 334	1 428	75	24,0
FIS	354, 1	816	20	6,4
BIIS	100, 1	535	5	1,8
Totalt	1 788, 2	2 779	100	32,2

Table S5. Estimated Quaternary sediment volumes and sediment rates in the main depocentres along the EurIS marine margin. For location see Fig. 1.

Region	Depositional area (10^3 km^2)	Sediment volume (10^3 km^3)	Maximum thickness (m)	Average thickness (m)	Maximum rate (cm/kyr)	Average rate (cm/kyr)	Delineated by contour (m)
North Nansen Basin	278	299	2300	1080	88	41	200
South Nansen Basin	128	80	1250	623	48	24	200
Fram Strait	13	3	590	241	23	9	200
Svalbard Margin	16	18	1680	1090	65	42	200
Storfjorden TMF	56	102	4500	1780	173	69	200
Bjørnøya TMF	281	379	3600	1340	140	52	200
Mid Norwegian margin	114	58	1500	517	58	20	200
North Sea TMF	64	47	1700	734	65	28	200
Norway Basin	155	68	1300	442	50	17	200
North Sea	203	81	1057	400	41	15	200
British-Irish margin	528	11	252	220	10	8	0

Table S6. Estimated sedimentation rates along the EurIS marine margin.

Nansen Basin - North	Time period (Ma)	**45-34**	**34-20**	**20 - 0**	**Method**
Nikishin et al. (2018)	Thickness (m)	1650	1120	2000	Linear
Fig. 6a	Sed rate (cm/k.y.)	15	8	10	

Nansen Basin - South	Time period (Ma)	**2.7-1.5**	**1.5-0.7**	**0.7-0**	**Method**
Lasabuda et al (2018);	Thickness (m)				Average
Table 1	Sed rate (cm/k.y.)	20	77	12	

Nansen Basin – South	Time period (Ma)	**55-7**	**7-2.6**	**2.6-0**	**Method**
Geissler and Jokat (2004);	Thickness (m)	1500	1200	500	Linear
Fig. 11	Sed rate (cm/k.y.)	3	27	19	

Fram Strait	Time period (Ma)	**35-7**	**7-2.6**	**2.6-0**	**Method**
Gebhardt et al. (2014);	Thickness (m)	1350	675	900	Linear
Fig 3	Sed rate (cm/k.y.)	5	15	35	

Sjurbrebanken TMF	Time period (Ma)	**5.8-2.6**	**2.6-1.5**	**1.5-0**	**Method**
Mattingsdal et al. (2014);	Thickness (m)	141	394	56	Linear
Fig. 6	Sed rate (cm/k.y.)	5	36	4	

Kongsfjorden TMF	Time period (Ma)	**5.8-2.6**	**2.6-1.5**	**1.5-0**	**Method**
Mattingsdal et al. (2014);	Thickness (m)	169	197	338	Linear
Fig. 6	Sed rate (cm/k.y.)	5	18	23	

Isfjorden TMF	Time period (Ma)	**1.5-0.78**	**0.78-0**	**Method**
Solheim et al. (1996);	Thickness (m)	800	100	Linear (isopach map)
Fig. 3	Sed rate (cm/k.y.)	111	13	

Isfjorden TMF	Time period (Ma)	**36-2.6**	**2.6-1.5**	**1.5-0.78**	**0.78-0**	**Method**
Amundsen et al. (2011);	Thickness (m)	600	400	700	100	Linear
Fig.3a	Sed rate (cm/k.y.)	2	36	97	13	

Bellsund TMF	Time period (Ma)	**1.5-0.78**	**0.78-0**	**Method**
Solheim et al. (1996);	Thickness (m)	1050	150	Linear (isopach map)
Fig. 3	Sed rate (cm/k.y.)	145	21	

Bellsund TMF Amundsen et al. (2011); Fig.6a	Time period (Ma)	**36-2.6**	**2.6-1.5**	**1.5-0.78**	**0.78-0**	**Method**
	Thickness (m)	1100	900	600	100	Linear
	Sed rate (cm/k.y.)	3	82	83	13	

Storfjorden TMF Hjelstuen et al. (1996); Table 2	Time period (Ma)	**36-2.6**	**2.6-1.5**	**1.5-0.78**	**0.78-0**	**Method**
	Thickness (m)	1100	813	705	110	Average
	Sed rate (cm/k.y.)	3	74	98	14	

Bjørnøyrenna TMF Fiedler & Faleide (1996); Fig. 5 (PQ), Table 2 (Q)	Time period (Ma)	**55-36**	**36-27**	**27-13**	**13-2.6**	**2.6-1.5**	**1.5-0.78**	**0.78-0**	**Method**
	Thickness (m)	804	670	804	335	478	964	196	PQ: Linear Q: Average
	Sed rate (cm/k.y.)	4	7	6	3	43	134	25	

Mid-Norwegian margin - outer Chand et al. (2011); Fig. 2	Time period (Ma)	**55-18**	**15-4**	**Method**
	Thickness (m)	960	660	Linear
	Sed rate (cm/k.y.)	3	6	

Mid-Norwegian margin - inner Chand et al. (2011); Fig. 2	Time period (Ma)	**55-18**	**15-4**	**Method**
	Thickness (m)	240	550	Linear
	Sed rate (cm/k.y.)	1	5	

Mid-Norwegian margin Dowdeswell et al (2010); Table 1	Time period (Ma)	**2.6-1.5**	**1.5-0.6**	**0.6-0.4**	**0.4-0.2**	**0.2-0**	**Method**
	Thickness (m)						Average
	Sed rate (cm/k.y.)	18	17	52	38	50	

North Sea TMF - proximal Q: Hjelstuen et al. (2012); Table 1 & Fig. 4 (deep area), this study. PQ: Stoker et al (2005), Fig. 6b.	Time period (Ma)	**23-2.6**	**2.6-1.1**	**1.1-0.5**	**0.5-0**	**Method**
	Thickness (m)	400	460*	134	800	PQ: Linear (isopach map)
	Sed rate (cm/k.y.)	2	30	22	162	Q: Average, *Linear, subtracting <1.1 Ma from total max thickness

North Sea TMF - distal Hjelstuen & Andreassen (2015); Fig. 4b.	Time period (Ma)	**36 - 2.6**	**2.6 - 0.5**	**0.5-0**	**Method**
	Thickness (m)	385	880	329	Linear
	Sed rate (cm/k.y.)	1	42	66	

North Sea Anell et al. (2012); Table 2	Time period (Ma)	**61-55**	**55-34**	**34-23**	**23-15**	**15-2.5**	**2.5-1.5**	**1.5-0**	**Method**
	Thickness (m)								Average
	Sed rate (cm/k.y.)	3,9	1,3	2,5	2,4	1	20	10	

North Sea Ottesen et al. (2018); Table 1	Time period (Ma)	**2.6-1.5**	**1.5-0.78**	**0.78-0**	**Method**
	Thickness (m)	217	304	95	Average
	Sed rate (cm/k.y.)	18	42	12	

North Sea Reinardy et al. (2017); Table 2, Fig. 2, Fig. 12	Time period (Ma)	**2.0-1.5**	**1.5-1.2**	**1.2-0.2**	**0.2-0**	**Method**
	Thickness (m)	60	240	160	N/A	Linear
	Sed rate (cm/k.y.)	12	80	16	N/A	

UK-Irish margin Stoker et al. (2005); Fig 5	Time period (Ma)	**15-2.6**	**2.6-0**	**Method**
	Thickness (m)	400	400	Linear (isopach map)
	Sed rate (cm/k.y.)	3	16	

Table S7. Estimated sediment discharge (10^3 m^3/yr).

NE Svalbard Margin Lasabuda et al. (2018); Table 1	Time period (Ma)	**2.6-1.5**	**1.5-0.78**	**0.78-0**
	Volume (10^3 km^3)	11	17	1
	Depositional Area (10^3 km^2)	44	28	8
	Discharge (10^3 m^3/yr)	10000	23611	897

Storfjorden TMF Hjelstuen et al. (1996); Table 2	Time period (Ma)	**55 - 2.6**	**2.6-1.5**	**1.5 - 0.78**	**0.78 - 0**
	Volume (10^3 km^3)	115	56	52	8
	Depositional Area (10^3 km^2)	68	69,4	73,8	72,6
	Discharge (10^3 m^3/yr)	2195	51273	72222	10256

Bjørnøyrenna TMF Fielder and Faleide (1996); Table 2	Time period (Ma)	**55 - 2.6**	**2.6-1.5**	**1.5 - 0.78**	**0.78 - 0**
	Volume (10^3 km^3)	162	99	190	106
	Depositional Area (10^3 km^2)	137	207	207	207
	Discharge (10^3 m^3/yr)	3092	90000	263889	135897

Mid-Norwegian margin Dowdeswell et al. (2010); Table 1	Time period (Ma)	**2.6-1.5**	**1.5 - 0.6**	**0.6 - 0.4**	**0.4 - 0.2**	**0.2 - 0**
	Volume (10^3 km^3)	34	24	17,1	12,5	16,3
	Depositional Area (10^3 km^2)	163	163	163	163	163
	Discharge (10^3 m^3/yr)	30909	26667	85500	62500	81500

North Sea TMF Hjelstuen et al. (2012); Table 1, Fig. 4. Nygård et al. (2005); Table 1	Time period (Ma)	**1.1-0.5**	**0.5-0**
	Volume (10^3 km^3)	4,7	23,3
	Depositional Area (10^3 km^2)		
	Discharge (10^3 m^3/yr)	7833	46600

North Sea, Anell et al. (2012); Table 2	Time period (Ma)	**61-55**	**55-34**	**34-23**	**23-15**	**15-2.5**	**2.5-1.5**	**1.5-0**
	Volume (10^3 km^3)	82,3	96,1	87,9	57,4	50,5	56,8	51,4
	Depositional Area (10^3 km^2)							
	Discharge (10^3 m^3/yr)	13716	4574	7993	6379	4039	56839	34288

North Sea Ottesen et al. (2018); Table 1	Time period (Ma)	**2.6-1.5**	**1.5-0.78**	**0.78-0**
	Volume (10^3 km^3)	38,4	53,8	16,9
	Depositional Area (10^3 km^2)	177	177	177
	Discharge (10^3 m^3/yr)	34909	74722	21667

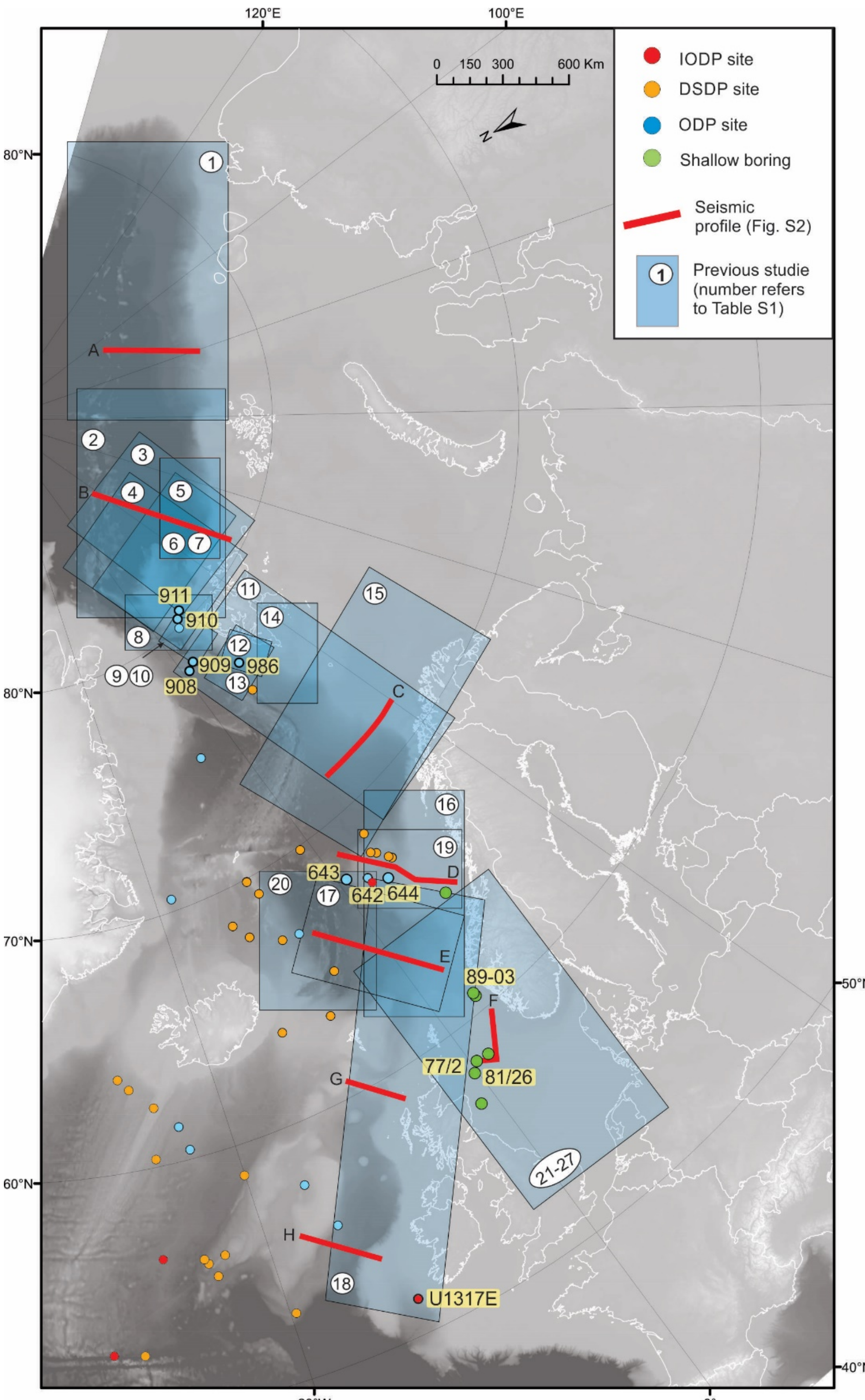

Figure S1. Overview of study areas in the published papers utilized in the present paper. Location of seismic profiles shown in Fig. S2, IODP-DSDP-ODP sites and shallow borings are shown.

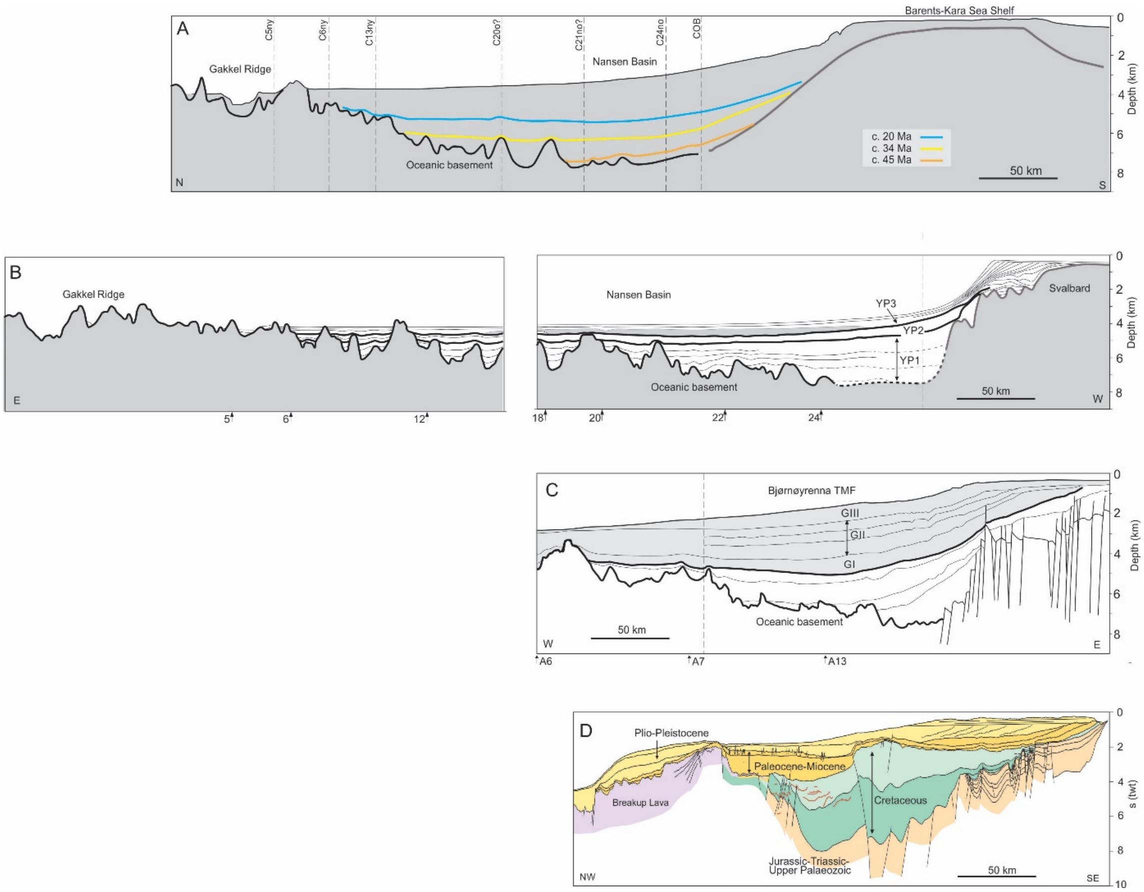

Figure S2. Line-drawing of seismic profiles showing typical geological settings along the paleo-EurIS marine margin. See Fig. S1 for profile location. **(A)** Northern Nansen Basin. COB: Continent-Ocean Boundary, C: Magnetic Cron (Modified from Nikishin et al. (2018)). **(B)** Southern Nansen Basin. YP1 (Eocene-Oligocene), YP2 (Miocene) YP3 (Pleistocene) are identified seismic units, A: Magnetic seafloor spreading anomalies (Modified from Jokat and Micksch (2004)), **(C)** Bjørnøyrenna TMF. GI (2.7-1.5 Ma), GII (1.5-0.7 Ma) and GIII (0.7-0 Ma) are identified seismic units. A: Magnetic seafloor spreading anomalies (Fiedler and Faleide, 1996). **(D)** Mid Norwegian margin (Modified from Blystad et al., 1995).

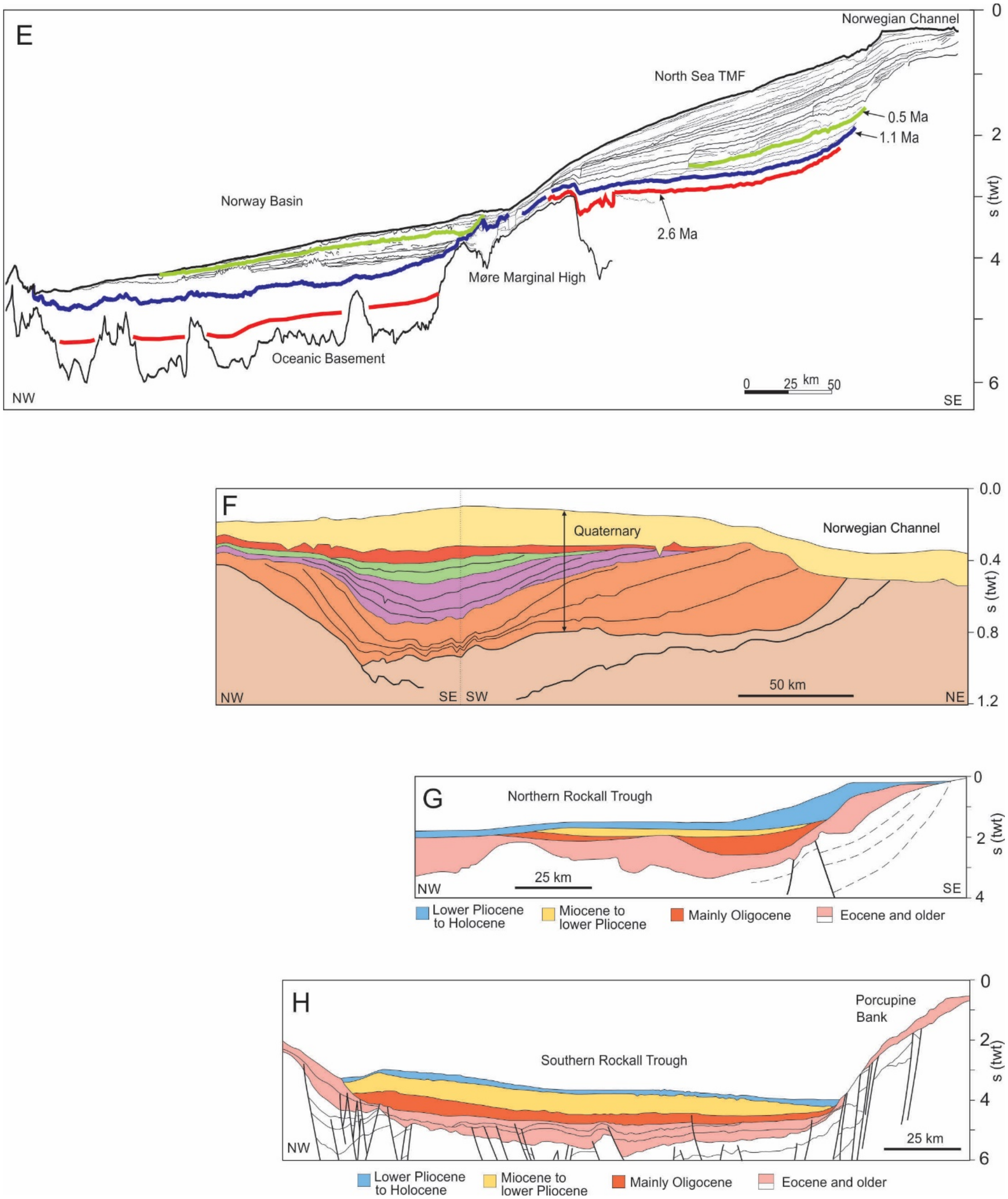

Figure S2 cont. **(E)** North Sea TMF and Norway Basin. (Modified from Hjelstuen et al. (2012)). **(F)** North Sea. (Modified from Baig (2018)), **(G)** British-Irish margin – north. (Modified from Stoker et al. (2005)), **(H)** British-Irish margin - south (Modified from Stoker et al., (2005)).

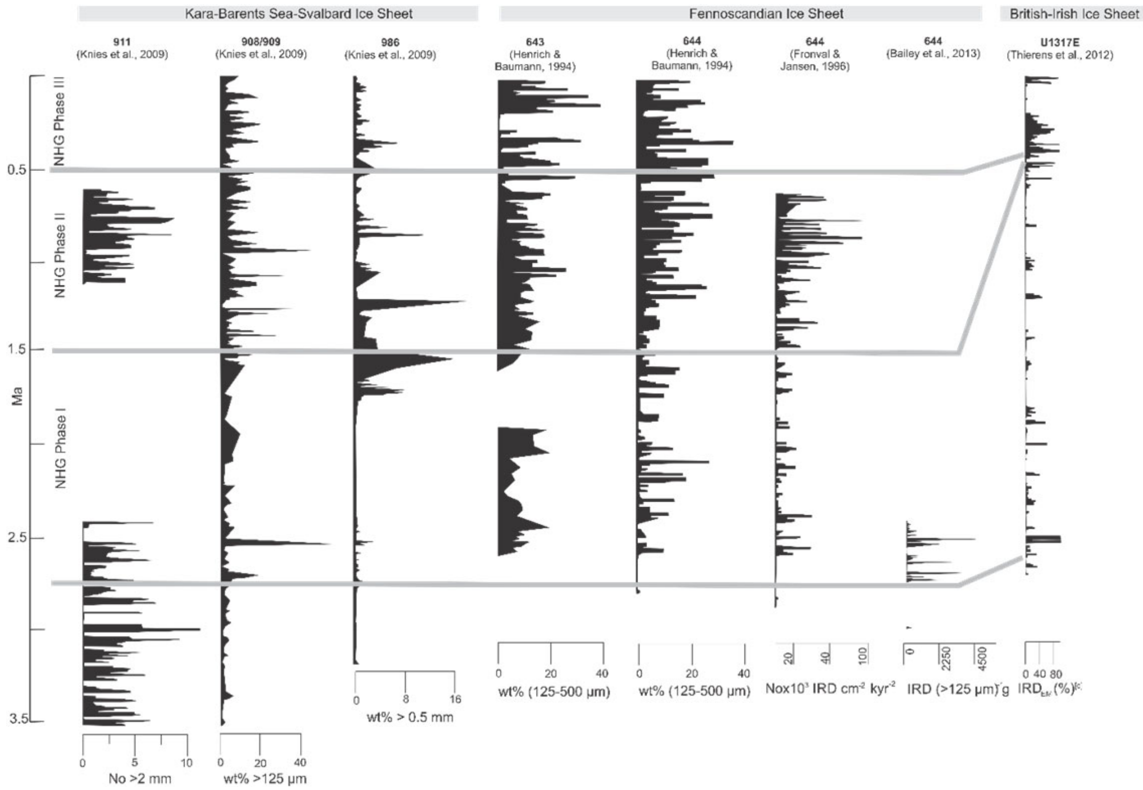

Figure S3. IRD records from the Svalbard, Mid-Norwegian and British-Irish margins. Location of ODP and IODP sites in Fig. S1. Compilation is based on Knies et al. (2009), Henrich and Baumann (1994), Fronval and Jansen (1996), Bailey et al. (2013) and Thierens et al. (2012).

REFERENCE CITED

Amundsen, I.M.H., Blinova, M., Hjelstuen, B.O., Mjelde, R., and Haflidason, H., 2011, The Cenozoic western Svalbard margin – sediment geometry and sedimentary processes in an area of ultraslow oceanic spreading: Marine Geophysical Research, v. 32, p. 441-453, DOI 10.1007/s11001-011-9127-z.

Anell, I., Thybo, H., and Rasmussen, E., 2012, A synthesis of Cenozoic sedimentation in the North Sea: Basin Research, v. 24, p. 154-179, https://doi.org/10.1111/j.1365-2117.2011.00517.x.

Baig, I., 2018. Burial and thermal histories of sediments in the southwestern Barents Sea and North Sea areas: evidence from integrated compaction, thermal maturity and seismic stratigraphic analyses. PhD thesis, University of Oslo, Department of Geosciences, 165 pp.

Bailey, I., Hole, G.M., Foster, G.L., Wilson, P.A., Storey, C.D., Trueman, C.N., and Raymo, M.E., 2013, An alternative suggestion for the Pliocene onset of major northern hemisphere glaciation based on the geochemical provenance of North Atlantic Ocean ice-rafted debris: Quaternary Science Reviews, v. 75, p. 181-194, https://doi.org/10.1016/j.quascirev.2013.06.004.

Blystad, P., Brekke, H., Færseth, R.B., Larsen, B.T., Skogseid, J., and Tørudbakken, B., 1995, Structural elements of the Norwegian continental shelf. Part II: The Norwegian Sea region: Norwegian Petroleum Directorate Bulletin, v. 8, 45 pp.

Chand, S., Rise, L., Knies, J., Haflidason, H., Hjelstuen, B.O., and Bøe, L., 2011, Stratigraphic development of the south Vøring Margin (Mid-Norway) since early Cenozoic time and its influence on subsurface fluid flow: Marine and Petroleum Geology, v. 28, p. 1350-1363, https://doi.org/10.1016/j.marpetgeo.2011.01.005.

Channell, J.E.T., Smelror, M., Jansen, E., Higgins, S., Lehman, B., Eidvin, T., Solheim, A., 1999, Age models for glacial fan deposits off East Greenland and Svalbard (ODP Site 986 and Site 987). In: Raymo, M., Jansen, E., Blum, P., Herbert, T.D. (Eds.), Proceeding Ocean Drilling Program. Scientific Results, vol. 162, pp. 149–166. Ocean Drilling Program, College Station, TX. doi:10.2973/odp.proc.sr.162.008.1999

Dowdeswell, J.A., Ottesen, D., and Rise, L., 2010. Rates of sediment delivery from the Fennoscandian Ice Sheet through an ice age: Geology, v. 38, p. 3–6. doi: https://doi.org/10.1130/G25523.1

Eldholm, O., Thiede, J., Taylor, E., et al., 1987, Proceedings of the Ocean Drilling Program, Initial Reports, Leg 104, 1141 pp, Ocean Drilling Program, College Station, Texas, USA. doi:10.2973/odp.proc.ir.104.1987

Engen, Ø., Gjengedal, J.A., Faleide, J.I., Kristoffersen, Y., and Eldholm, O., 2009, Seismic stratigraphy and sediment thickness of the Nansen Basin, Arctic Ocean: Geophysical Journal International, v. 176, p. 805–821, https://doi.org/10.1111/j.1365-246X.2008.04028.x.

Faleide, J.I., Solheim, A., Fiedler, A., Hjelstuen, B.O., Andersen, E.S., and Vanneste, K., 1996, Late Cenozoic evolution of the western Barents Sea-Svalbard continental margin: Global and Planetary Change, v. 12, p. 53-74, https://doi.org/10.1016/0921-8181(95)00012-7.

Fiedler, A., and Faleide, J.I., 1996, Cenozoic sedimentation along the southwestern Barents Sea margin in relation to erosion and uplift of the shelf: v. 12, p. 75-93, https://doi.org/10.1016/0921-8181(95)00013-5.

Fransner, O., Noormets, R., Flink, A.E., Hogan, K.A., Dowdeswell, J.A., 2018, Sedimentary processes on the continental slope off Kvitøya and Albertini troughs north of Nordaustlandet, Svalbard – The importance of structural-geological setting in trough-mouth fan development: Marine Geology, v. 402, p. 194-208, https://doi.org/10.1016/j.margeo.2017.10.008.

Fronval, T., and Jansen, E., 1996, Late Neogene paleoclimates and paleoceanography in the Iceland-Norwegian Sea: Evidence from the Iceland and Vøring Plateau. In: Thiede, J., et al., Proceedings of the Ocean Drilling Program, Scientific Results, v. 151, p. 455-468.

Gebhardt, A.C., Geissler, W.H., Matthiessen, J., and Jokat, W., 2014, Changes in current patterns in the Fram Strait at the Pliocene/Pleistocene boundary: Quaternary Science Reviews, v. 92, p. 179-189, https://doi.org/10.1016/j.quascirev.2013.07.015.

Geissler, W. H., Jokat, W., and Brekke, H., 2011. The Yermak Plateau in the Arctic Ocean in the light of reflection seismic data-implication for its tectonic and sedimentary evolution: Geophysical Journal International, v. 187, p. 1334-1362, https://doi.org/10.1111/j.1365-246X.2011.05197.x.

Geissler, W.H., and Jokat, W., 2004, A geophysical study of the northern Svalbard continental margin. Geophysical Journal International, v. 158, p. 50–66, https://doi.org/10.1111/j.1365-246X.2004.02315.x.

Henrich, R., and Baumann, K.-H., 1994, Evolution of the Norwegian Current and the Scandinavian Ice Sheets during the past 2.6 m.y.: evidence from ODP Leg 104 biogenic carbonat and terrigenous records: Palaeogeography, Palaeoclimatology, Palaeoecology, v. 108, p. 75-94, https://doi.org/10.1016/0031-0182(94)90023-X.

Hjelstuen, B.O., and Andreassen, E.V, 2015, North Atlantic deep water processes and depositional environments: A study of the Cenozoic Norway Basin: Marine and Petroleum Geology, v. 59, p. 429-441, https://doi.org/10.1016/j.marpetgeo.2014.09.011.

Hjelstuen, B.O., Elverhøi, A., and Faleide, J.I., 1996, Cenozoic erosion and sediment yield in the drainage area of the Storfjorden Fan: Global and Planetary Change, v. 12, p. 95-117, https://doi.org/10.1016/0921-8181(95)00014-3.

Hjelstuen, B.O., and Grinde, S., 2016, 3D seismic investigation of Pleistocene Mass Transport Deposits and Glacigenic Debris Flows on the North Sea Fan, NE Atlantic Margin. In: Lamarche, G et al. (eds) Submarine Mass Movements and Their Consequences, Advances in Natural and Technological Hazard Research, pp 265-272.

Hjelstuen, B.O., Nygård, A., Sejrup, H.P., and Haflidason, H., 2012, Quaternary denudation of southern Fennoscandia - evidence from the marine realm: Boreas, v. 41, p. 379-390, https://doi.org/10.1111/j.1502-3885.2011.00239.x.

Jokat, W., and Micksch, U., 2004. Sedimentary structure of the Nansen and Amundsen basins, Arctic Ocean: Geophysical Research Letter, v. 31, L02603, doi: 10.1029/2003GL018352.

Knies, J., Matthiessen, J., Vogt, C., Laberg, J.S., Hjelstuen, B.O., Smelror, M., Larsen, E., Andreassen, K., Eidvin, T., and Vorren, T., 2009, The Plio-Pleistocene glaciations of the Barents Sea-Svalbard region: a new model based on revised chronostratigraphy: Quaternary Science Reviews, v. 28, p. 812-829, https://doi.org/10.1016/j.quascirev.2008.12.002.

Kuhlmann, G., Langereis, C., Munsterman, D., van Leeuwen, R.J., Verreussel, R., Meulenkamp, J., Wong, T., 2006, Chronostratigraphy of Late Neogene sediments in the southern North Sea Basin and paleoenvironmental interpretations: Palaeogeography, Palaeoclimatology, Palaeoecology, v. 239, p. 426-455, https://doi.org/10.1016/j.palaeo.2006.02.004.

Laberg, J.S., Andreassen, K., Knies, J., Vorren, T.O., and Winsborrow, M., 2010, Late Pliocene–Pleistocene development of the Barents Sea Ice Sheet: Geology, v. 38, p. 107–110, https://doi.org/10.1130/G30193.1.

Laberg, J.S., Andreassen, K., and Vorren, T.O., 2012, Late Cenozoic erosion of the high-latitude southwestern Barents Sea shelf revisited: Geological Society American Bulletin, v. 124, p. 77-99, https://doi.org/10.1130/B30340.1.

Lasabuda, A., Geissler, W. H., Laberg, J. S., Knutsen, S.□M., Rydningen, T.A., and Berglar, K., 2018, Late Cenozoic erosion estimates for the northern Barents Sea: Quantifying glacial sediment input to the Arctic Ocean: Geochemistry, Geophysics, Geosystems, v. 19, p. 4876– 4903, https://doi.org/10.1029/2018GC007882.

Mattingsdal, R., Knies, J., Andreassen, K., Fabian, K., Husum, K., Grøsfjeld, K., and De Schepper, S., 2014, A new 6 Myr stratigraphic framework for the Atlantic–Arctic Gateway: Quaternary Science Reviews, v. 92, p. 170-178, https://doi.org/10.1016/j.quascirev.2013.08.022.

Montelli, M., Dowdeswell, J.A., Ottesen, D., and Johansen, S.E., 2017, Ice-sheet dynamics through the Quaternary on the mid-Norwegian continental margin inferred from 3D seismic data: Marine and Petroleum Geology, v. 80, p. 228-242, https://doi.org/10.1016/j.marpetgeo.2016.12.002.

Myhre, A., Thiede, J., Firth, J.A. (Eds.), 1995, Proceedings of the Ocean Drilling Program. Initial Reports, Leg 151, 951 pp. Ocean Drilling Program, College Station, Texas, USA, doi:10.2973/odp.proc.ir.151.1995.

Nikishin, A.M., Gaina, C., Petrov, E.I., Malyshev, N.A., and Freiman. S.I., 2018, Eurasia Basin and Gakkel Ridge, Arctic Ocean: Crustal asymmetry, ultra-slow spreading and continental rifting revealed by new seismic data: Tectonophysics, v. 746, p. 64-82, https://doi.org/10.1016/j.tecto.2017.09.006.

Nygård, A., Sejrup, H.P., Haflidason, H., and Bryn, P., 2005, The glacial North Sea Fan, southern Norwegian Margin: architecture and evolution from the upper continental slope to the deep-sea basin: Marine and Petroleum Geology, v. 22, p. 71-84, https://doi.org/10.1016/j.marpetgeo.2004.12.001.

Ottesen, D., Batchelor, C.L., Dowdeswell, J.A., and Løseth, H., 2018, Morphology and pattern of Quaternary sedimentation in the North Sea Basin (52–62°N): Marine and Petroleum Geology, v. 98, p. 836-859, https://doi.org/10.1016/j.marpetgeo.2018.08.022.

Ottesen, D., Dowdeswell, J.A., Rise, L., and Bugge, T., 2012, Large-scale development of the mid-Norwegian shelf over the last three million years and potential for hydrocarbon reservoirs in glacial sediments: Geological Society, London, Special Publications, v. 368, p. 53-73, https://doi.org/10.1144/SP368.6.

Rea, B.R., Newton, A.M.W., Lamb, R.M., Harding, R., Bigg, G.R., Rose, P., Spagnolo, M., Huuse, M., Cater, John M.L., Archer, S., Buckley, F., Halliyeva, M., Huuse, J., Cornwell, D.G., Brocklehurst, S.H., Howell, J.A., Extensive marine-terminating ice sheets in Europe from 2.5 million years ago, 2018, v. 4., 11 pp., 10.1126/sciadv.aar8327

Reinardy, B.T.I., Hjelstuen, B.O., Sejrup, H.P., Augedal, H., and Jørstad, A., 2017, Late Pliocene-Pleistocene environments and glacial history of the northern North Sea: Quaternary Science Reviews, v. 158, p. 107-126, https://doi.org/10.1016/j.quascirev.2016.12.022.

Reinardy, B.T.I., Sejrup, H.P., Hjelstuen, B.O., King, E., and Augedal, H., 2018, A Quaternary aminostratigraphy constraining chronology of depositional environments in the North Sea Basin: Marine Geology, v. 402, p. 139-152, https://doi.org/10.1016/j.margeo.2017.11.004.

Rise, L., Ottesen, D., Longva, O., Solheim, A., Andersen, E.S., and Ayers, S., 2006, The Sklinnadjupet slide and its relation to the Elsterian glaciation on the mid-Norwegian margin: Marine and Petroleum Geology, v. 23, p. 569-583, https://doi.org/10.1016/j.marpetgeo.2006.05.005.

Sarkar, S., C., Chabert, A., Masson, D.G., Minshull, T.A., and Westbrook, and G.K., 2011, Switching of a paleo-ice stream in northwest Svalbard: Quaternary Science Reviews, v. 30, p. 1710-1725, https://doi.org/10.1016/j.quascirev.2011.03.013.

Sejrup, H. P., E. Larsen, J. Landvik, E. L. King, H. Haflidason, and A. Nesje, 2000, Quaternary glaciations in southern Fennoscandia: evidence from southwestern Norway and the northern North Sea region: Quaternary Science Reviews, v. 19, p. 667-685, https://doi.org/10.1016/S0277-3791(99)00016-5.

Sejrup, H. P., I. Aarseth, H. Haflidason, R. Løvlie, Å. Bratten, G. Tjøstheim, C. F. Forsberg, and K. I. Ellingsen, 1995, Quaternary of the Norwegian Channel: glaciation history and palaeoceanography: Norsk Geologisk Tidsskrift, v. 75, p. 65-87.

Sejrup, H. P., I. Aarseth, K. L. Ellingsen, E. Reither, E. Jansen, R. Løvlie, A. Bent, J. Brigham-Grette, E. Larsen, and M. Stoker, 1987, Quaternary stratigraphy of the Fladen area, central North Sea: A multidisciplinary study: Journal of Quaternary Science, v. 2, p. 35-58, https://doi.org/10.1002/jqs.3390020105.

Solheim, A., Andersen, E.S., Elverhøi, A., and Fiedler, A., 1996, Late Cenozoic depositional history of the western Svalbard continental shelf, controlled by subsidence and climate, Global and Planetary Change, v. 12, 135–148, https://doi.org/10.1016/0921-8181(95)00016-X.

Solheim, A., Faleide, J.I., Andersen, E.S., Elverhøi, A., Forsberg, C.F., Vanneste, K., Uenzelmann-Neben, G., and Channell, J.E.T., 1998, Late Cenozoic seismic stratigraphy and glacial geological development of the Svalbard-Barents Sea continental margins. Quaternary Science Review, v. 17, p. 155-184, https://doi.org/10.1016/S0277-3791(97)00068-1.

Stoker, M.S., Praeg, D., Hjelstuen, B.O., Laberg, J.S., Nielsen, T., and Shannon, P.M., 2005, Neogene stratigraphy and the sedimentary and oceanographic development of the NW

European Atlantic margin: Marine and Petroleum Geology, v. 22, p 977-1005, https://doi.org/10.1016/j.marpetgeo.2004.11.007.

Stoker, M.S., Skinner, A.C., Fyfe, J.A., Long, D., 1983, Paleomagnetic evidence for early Pleistocene in the central and northern North Sea. Nature, v. 304, p. 332-334.

Thierens, M., Pirlet, H., Colin, C., Latruwe, K., Vanhaecke, F., Lee, J.R., Stuut, J.-B., Titschack, J., Huvenne, V.A.I., Dorschel, B., Wheeler, A.J., and Henriet, J.-P., 2012, Ice-rafting from the British–Irish ice sheet since the earliest Pleistocene (2.6 million years ago): implications for long-term mid-latitudinal ice-sheet growth in the North Atlantic region: Quaternary Science Reviews, v. 44, p. 229-240, https://doi.org/10.1016/j.quascirev.2010.12.020.

Waage, M., Bünz, S., Bøe, R., and Mienert, J., 2018, High-resolution 3D seismic exhibits new insights into the middle-late Pleistocene stratigraphic evolution and sedimentary processes of the Bear Island trough mouth fan: Marine Geology, v. 403, p. 139-149, https://doi.org/10.1016/j.margeo.2018.05.006.